Collapse behaviors of plane lattice arches under excessive dynamic and static vertical loads

Yoshiya TANIGUCHI*, Risa FUKUSHIMA[a], Susumu YOSHINAKA[b]

*Professor, Graduate School of Osaka City University
Sugimoto 3-3-138, Sumiyoshi-ku, Osaka 5588585, Japan
ytaniguchi@arch.eng.osaka-cu.ac.jp

[a] Graduate School of Osaka City University
[b] Lecturer, Graduate School of Osaka City University

Abstract

The public buildings such as gymnasiums which are realized with spatial structures have been often used for regional temporary shelters when the disaster of huge earthquakes or typhoons has occurred. Therefore, the safety of spatial structures may be important for the disaster prevention plan. Then in this paper as for simple lattice structures, dynamic collapse behavior and static collapse behavior are numerically estimated in order to investigate what physical quantity is the definite factor that determines the load level of dynamic collapse, that is, the correlation of the two collapse phenomena. It has been pointed out that a physical quantity is the strain energy of structures [1, 5]. In the dynamic simulations, the collapse is recognized by a sudden increase of the monitored nodal displacements and the maximum input acceleration values of earthquakes are gradually increased while monitoring the maximum displacements. As the results, an estimation method is presented to predict the collapse level of vertical seismic motions with the information of static collapse behavior of structures.

Keywords: plane lattice arch, dynamic collapse, elasto-plastic behavior, equivalent velocity of strain energy, velocity response spectrum, earthquake input energy

1. Introduction

Seismic resistant capacities for long span structures have been studied by many researchers all over the world. Among them early on, Kato et al. [2] studied the static and dynamic behaviors of long span beams against vertical loads to express the quantitative earthquake resistant capacity in terms of the first natural period and the slenderness ratio of upper chord members. The peak ground acceleration at dynamic collapse was selected for the measured standard. Murata [3] examined the collapse maximum input acceleration while the static safety rate was changed for single-layer lattice domes. Ogawa et al. [4] examined an effect of the dynamic impulse load to give to the buckling collapse property of the single-layer lattice domes and showed about 20% reduction from the static load-carrying capacity. Tada et al. [5] introduced the gravity energy defined by the product of the self

weight and the vertical displacement, into the input energy as a collapse index for double-layer grids. It was shown that the double-layer grid began to collapse when the seismic input energy of the grid exceeded a certain amount. Qiao et al. [6] investigated the dynamic collapse behavior of a single layer shallow lattice dome to make clear the relations between the maximum absorbed energies and the vibration modes and pointed out that the maximum absorbed energies were different with different vibration modes. Taniguchi et al. [1] investigated the earthquake input energy at dynamic collapse for double-layer structures and showed that the pseudo velocity responses corresponding to the large effective mass modes were related to the equivalent velocity corresponding to the earthquake input energy by a time history analysis.

In this paper, numerical studies are carried out with the input energy index to make the relation between a dynamic collapse property and a static elasto-plastic (collapse) behavior under excessive vertical loads, for a plane lattice arch. The estimation method is presented that the dynamic collapse level of ground motions is predicted with the performances of a static elasto-plastic analysis, a free vibration analysis, and a pseudo-velocity response spectrum of seismic motions. It is noted that the present method is based on the extrapolation method.
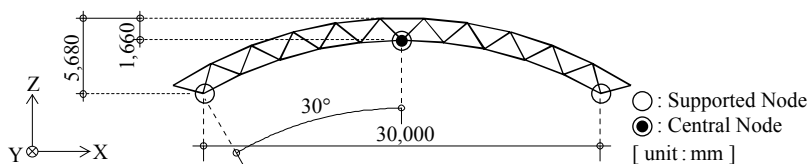
2. Plane lattice arch

Figure 1: Plane lattice arch

Table 1: Mechanical and sectional properties of member

Model	Section Size $\phi \times t$ (mm)	Cross Section Area A (mm^2)	Geometrical Moment of Inertia I (mm^4)	Slenderness Ratio λ
P1	89.1 × 3.2	864	7.98×10^5	77-109
P2	60.5 × 3.2	576	2.37×10^5	116
	76.3 × 3.2	735	4.92×10^5	121-128
	89.1 × 3.2	864	7.98×10^5	103
	89.1 × 4.5	1200	1.07×10^6	105
PR1	114.3 × 4.5	1550	2.34×10^6	60-85
PR2	60.5 × 3.2	576	2.37×10^5	116
	76.3 × 3.2	735	4.92×10^5	91-128
	89.1 × 3.2	864	7.98×10^5	103-109
	114.3 × 3.2	1120	1.72×10^6	84
	114.3 × 4.5	1550	2.34×10^6	85
Young's Modulus E (MPa)	2.05×10^5		Yield Stress σ_y (MPa)	300

The numerical analysis models are a plane lattice arch as shown in Figure 1. The joints of models are assumed to be rigid. Two support conditions are considered. In this paper, the letter P in model names denotes the pin-support condition and PR denotes the pin-roller-support condition. Mechanical and sectional properties of members are shown in Table 1. The constituent members of lattice arch are designed by the allowable stress design method. The letter 1 in model names denotes that all members are the same sections and 2 denotes that the models consist of several kinds of members.

3. Static elasto-plastic behavior

The static elasto-plastic behaviors are investigated theoretically. The numerical analysis method is a static elasto-plastic analysis taking into account the geometrical and material nonlinearities. All nodes of the upper layer are subjected to uniform distributed loads.
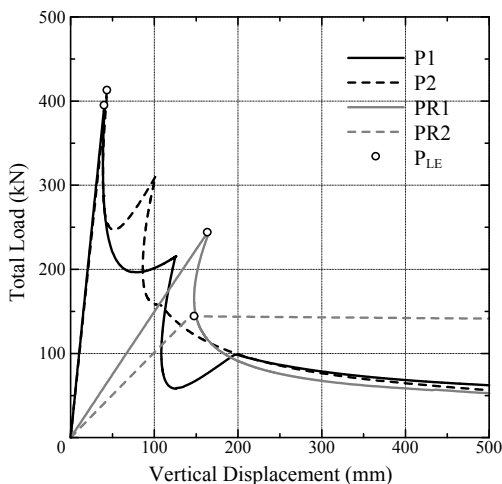

Figure 2: Load-deflection relationships

The results obtained are shown in Figures 2, 3 and Table 2. Figure 2 shows the relationships between the total load and the vertical displacement of the central node as shown in Figure 1. P_{LE} is the elastic limit load at which at least one or more members are yielded. The load-deflection relationships after the peaks are generally decreasing for the models, except for PR2 model. The PR2 model conserves the load bearing capacity after the limit load, since the center lower chord members are yielded in tension.

Figure 3 shows the relationships between the vertical displacement of central node and equivalent velocities of energies. In a static analysis, the energy balance is expressed as follows.

$$E_E - E_G = E_F \tag{1}$$

where E_E is the strain energy, E_G is the potential energy performed by the dead load and the vertical displacement, E_F is the input energy by the external vertical loads. Then E_F can be called as the static absorbed energy of system. These three values are converted respectively to velocity expressions as follows.

$$_sV = \sqrt{2E_E/M}, \quad _sV^G = \sqrt{2E_G/M}, \quad _sV^F = \sqrt{2E_F/M} \tag{2a,b,c}$$

where M is the mass of models. In this paper, $_sV_f$ represents the equivalent velocity of the strain energy E_E at the maximum value of static absorbed energy $_sV^F$. The value at the initial yield is defined as $_sV_{LE}$. Table 2 shows these values with the dead load and the initial yield load. As for PR2 model, the absorbed energy $_sV^F$ doesn't reach the peak, the value when the largest extensional strain of members exceeds 3% is adopted as $_sV_f$.
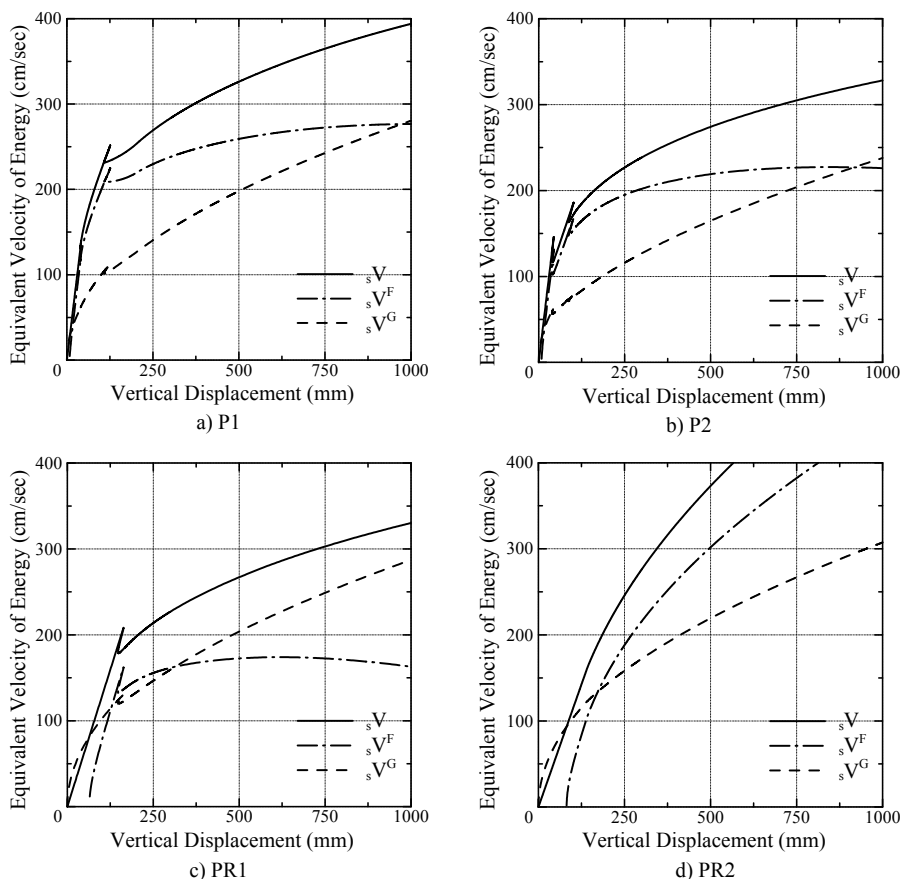

Figure 3: Relationships between vertical displacement and equivalent velocity of energy

Table 2: Elastic limit load and equivalent velocity of strain energy
at elastic limit and maximum static absorbed energy

Model	Dead Load P_{DL} (kN)	Elastic Limit Load P_{LE} (kN)	$_sV_{LE}$ (cm/sec)	$_sV_f$ (cm/sec)	$_sV_f/_sV_{LE}$
P1	40.8	395	134	399	2.98
P2	39.3	413	146	315	2.15
PR1	47.1	244	207	286	1.38
PR2	40.5	144	168	548*	3.27

* : the value at the extensional strain exceeds 3%

4. Free vibration behavior

Free vibration analyses without any damping are carried out. The effective mass ratios of large 3 values in each direction are shown in Table 3. These values of Z direction in Table 3 are used in chapter 6 to estimate the initial yield level.

Table 3: Natural period and effective mass ratio

a) P1

Mode Number	Natural Period (sec)	X-Direction		Z-Direction	
1	0.1412	38.78	1	0.00	
2	0.1152	0.00		57.19	1
3	0.0568	0.00		9.32	3
4	0.0475	36.67	2	0.00	
5	0.0328	9.99	3	0.00	
8	0.0237	0.00		16.82	2
Total 30 mode of Effective Mass Ratio (%)		99.98		100.00	

b) P2

Mode Number	Natural Period (sec)	X-Direction		Z-Direction	
1	0.1485	35.62	1	0.00	
2	0.1147	0.00		55.40	1
3	0.0619	0.00		10.13	3
4	0.0476	31.35	2	0.00	
5	0.0353	16.80	3	0.00	
8	0.0268	0.00		21.30	2
Total 30 mode of Effective Mass Ratio (%)		99.94		100.00	

c) PR1

Mode Number	Natural Period (sec)	X-Direction		Z-Direction	
1	0.3973	31.38	1	43.14	1
2	0.1104	26.88	2	8.62	
3	0.0559	26.29	3	5.44	
4	0.0451	4.10		10.99	3
9	0.0184	0.13		14.20	2
Total 30 mode of Effective Mass Ratio (%)		99.98		99.98	

d) PR2

Mode Number	Natural Period (sec)	X-Direction		Z-Direction	
1	0.4605	34.00	1	41.20	1
2	0.1369	27.36	2	10.09	
3	0.0695	21.12	3	3.94	
4	0.0549	8.07		14.19	3
8	0.0165	0.00		14.82	2
Total 30 mode of Effective Mass Ratio (%)		99.99		100.00	

5. Dynamic elasto-plastic behavior

5.1. Numerical analysis condition

The dynamic elasto-plastic behaviors are estimated by the educational analysis software SPACE [7]. The numerical integration scheme is the Newmark-β method, and the value of β is 0.25. The time increment δ_t is 0.001 second, which is about 1/100 of the natural period for the mode of the maximum effective mass ratio. Rayleigh damping is used and the damping ratios for two modes of the large effective mass ratio are 0.02.

The input seismic waves are the observed motion; Kobe 1995, and the artificial wave; BCJ (The Building Center of Japan) level 2. The component of Kobe is UD (Up and Down). The input direction of seismic waves is z-direction.

The dynamic collapse is recognized by a sudden increase of monitored nodal displacements. The monitored node is the central node as shown in Figure 1. The threshold level of collapse is 1,000mm in the present work.

5.2. Initial yield acceleration and dynamic collapse acceleration

The initial yield accelerations A_{LE} and the dynamic collapse accelerations A_f are shown in Table 4. Each value in the table is corresponding to the maximum input acceleration of seismic motions when the model becomes inelastic or shows the dynamic collapse behavior. The ratios of A_f / A_{LE} are distributed within the range of 1.1-1.4 except for PR2 model, but the value is large for PR2. It depends on the load bearing capacities after the peak loads as shown in Figure 3.

Table 4: Maximum input acceleration at initial yield and dynamic collapse

Model	A_{LE} (cm/sec^2)		A_f (cm/sec^2)		A_f/ A_{LE}	
	BCJ-L2	KOBE	BCJ-L2	KOBE	BCJ-L2	KOBE
P1	3960	3300	5690	4370	1.44	1.32
P2	3990	3300	5030	3620	1.26	1.10
PR1	1060	1140	1170	1590	1.10	1.39
PR2	520	1090	1420	4050	2.73	3.72

5.3. Earthquake input energy

In this section, the earthquake input energies of arches are estimated at the two stages of initial yield and dynamic collapse. The earthquake input energy is defined as the maximum response of the sum of elastic strain energy and the energy dissipated by plastic deformation during the time history analyses [8]. The energy obtained is converted into the equivalent velocity V_{LE} and V_f respectively. These values are shown in Table 5. In the table, the ratios V_f / V_{LE} are distributed within the range of 1.0 to 3.7 except for PR2 model.

The distribution range of Table 5 is larger than that of Table 4. It is different from the result in Ref.1. It is the reason that the collapse is recognized by a sudden increase of the monitored nodal displacements and the collapse mechanism may be not formed in fact.

Table 5: Equivalent velocity of energy at initial yield and dynamic collapse

Model	V_{LE} (cm/sec)		V_f (cm/sec)		V_f/V_{LE}	
	BCJ-L2	KOBE	BCJ-L2	KOBE	BCJ-L2	KOBE
P1	142	142	529	317	3.73	2.23
P2	143	147	146	237	1.02	1.61
PR1	207	201	224	263	1.08	1.31
PR2	154	150	514	658	3.34	4.39

The relationships between the ratios $_sV_f$ / $_sV_{LE}$ obtained by the static elasto-plastic analysis and the ratios V_f / V_{LE} obtained by the time history response analysis are plotted as shown in Figure 4. The solid line in this figure is the regression line given by the least-square approximation. The slope of regression line is about 1 in spite of the difference of the seismic motions. It means that the absorbed strain energy of system is related to the dynamic collapse.
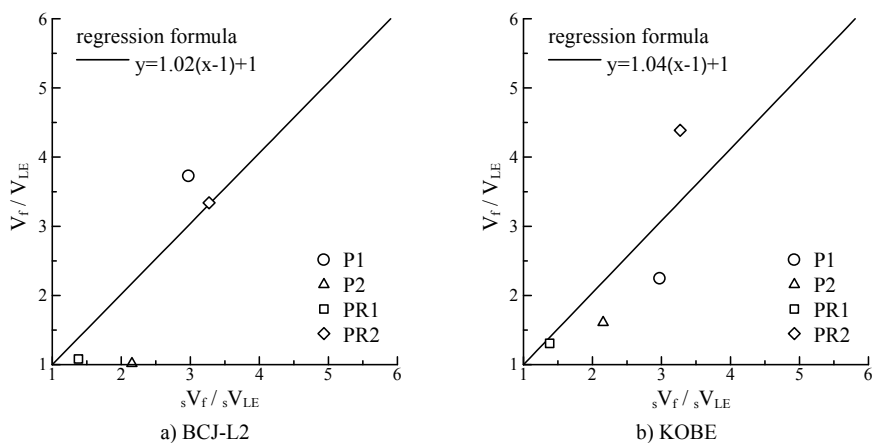

Figure 4: Relationships between dynamic and static behavior

6. Estimation method of dynamic collapse level

In this chapter, the initial yield and the dynamic collapse level are estimated with pseudo velocity response spectrum. Figure 5 shows the response spectrum at initial yield and the effective mass ratio. The dotted and dashed line represents the level of the earthquake input energy V_{LE} by the time history analyses. The sum of the velocity responses corresponding to the large 3 effective mass modes in the Z direction is the approximate value denoted as $V_{LE}*$. The comparison between the approximate value $V_{LE}*$ and the exact value V_{LE} is shown in Table 6 and Figure 6.
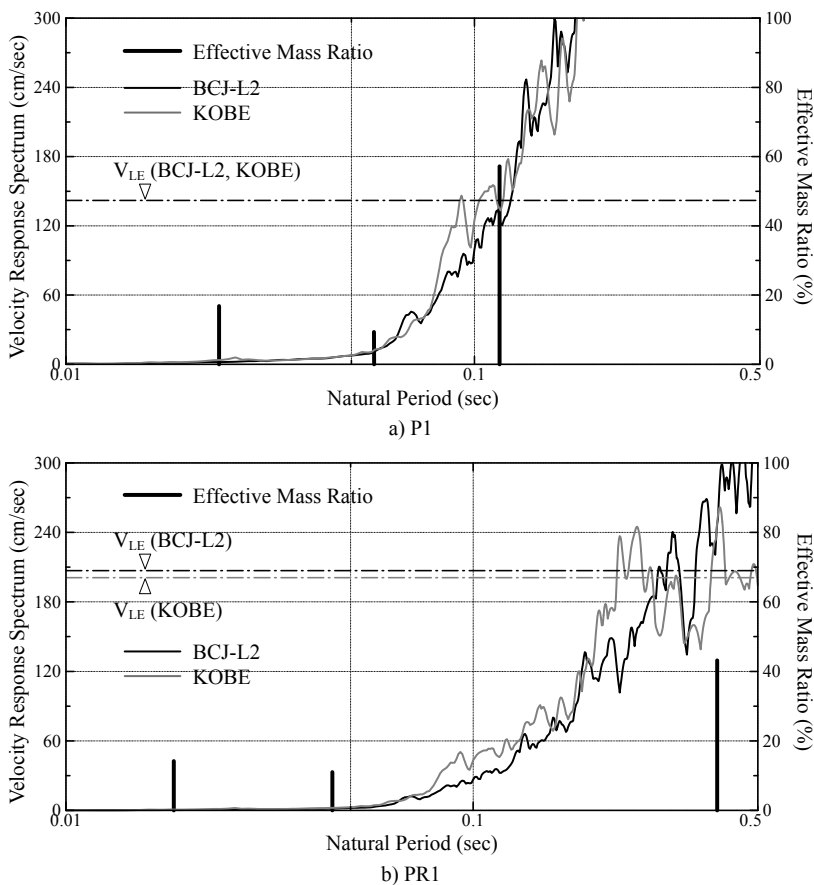
Figure 5: Pseudo-velocity response spectrum at initial yield and effective mass ratio

Table 6: Estimation of equivalent velocity of earthquake input energy at initial yield

Seismic Wave	Model	V_{LE} (cm/sec)	V_{LE}^* (cm/sec)	V_{LE}^*/V_{LE}		
				V_{LE}^*/V_{LE}	Mean Value	Standard Deviation
BCJ-L2	P1	142	143	1.01		
	P2	143	152	1.06	1.07	0.07
	PR1	207	248	1.20		
	PR2	154	158	1.03		
KOBE	P1	142	151	1.07		
	P2	147	161	1.10	1.17	0.09
	PR1	201	250	1.24		
	PR2	150	189	1.26		

By using an extrapolation method, the approximate value V_f* of dynamic collapse level is estimated with the regression formula in Figure 4 and one more approximate value $V_{LE}*$. The ratios V_f* / V_f and the accuracy are shown in Table 7 and Figure 7.

Table 7: Estimation of equivalent velocity of earthquake input energy at dynamic collapse

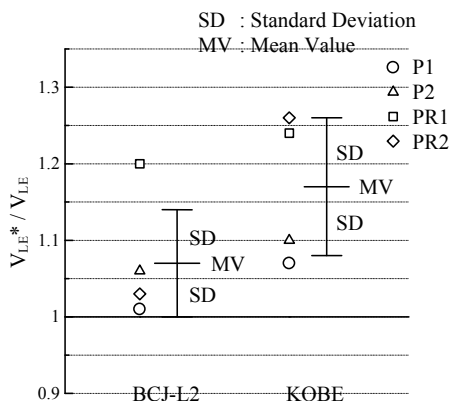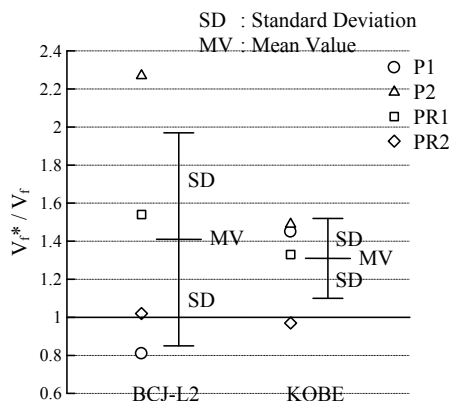| Seismic Wave	Model	V_f (cm/sec)	V_f* (cm/sec)	V_f*/V_f		
				V_f*/V_f	Mean Value	Standard Deviation
BCJ-L2	P1	529	431	0.81		
	P2	146	331	2.27	1.41	0.56
	PR1	224	344	1.54		
	PR2	514	524	1.02		
KOBE	P1	317	461	1.45		
	P2	237	354	1.49	1.31	0.21
	PR1	263	349	1.33		
	PR2	658	636	0.97		

Figure 6: Estimate accuracy
for initial yield

Figure 7: Estimate accuracy
for dynamic collapse

Figure 7 shows that the accuracy is not so good in the estimation of the dynamic collapse level than Figure 6 of the initial yield level. Although the value of V_f* / V_f is 2.27 as for P2 model under BCJ-L2, the other models are about 0.8-1.5. It should be noted again that the value V_f of P2 model is almost equal to the value of initial yield since the true collapse mechanism may not be formed.

7. Conclusions

The estimation method with the information of static elasto-plastic behavior, free vibration behavior, and the pseudo velocity response spectrum of seismic motions is presented. In the present work, the accuracy of the prediction values is 0.8 – 2.3 in comparison with the result by the time history response analyses.

This paper has shown the possibility that the dynamic collapse strength of lattice structures against seismic motions could be estimated by a static elasto-plastic analysis as well as a complicated time history response analysis.

Acknowledgement

References

[1] Taniguchi, Y., Phillip L. Gould and Kurano, M., Earthquake input energy at dynamic collapse for double-layer cylindrical lattice roofs, *Journal of IASS*, Vol.49, pp.89-96, 2008.

[2] Kato, S., Ishikawa, K. and Yokoo, Y., Earthquake Resistant Capacity of Long Span Trusses Structures A Study on Trussed Beam due to Vertical Earthquake Motions, *Journal of Structural and Construction Engineering (Transactions of AIJ)*, No.360, pp.64-74, 1986.

[3] Murata, M., Dynamic Characteristics of Single Layer Reticular Domes subjected to Vertical and Horizontal Earthquake Motions, *Journal of Structural and Construction Engineering (Transactions of AIJ)*, No.571, pp.103-110, 2003.

[4] Ogawa T., Kumagai T. and Takemoto Yumi, The effect of shock motion on dynamic buckling behaviour of rigidly jointed single layer lattice domes, Extended Abstracts and CD-ROM of IASS International Symposium, Japan, TP089, 2001.

[5] Tada, M., Hayashi, M. and Yoneyama, T., An Improvement of Seismic Capacity of Double-Layer Space Trusses using Force Limiting Devices, *Spatial Structures: Heritage, Present and Future, Proc. of the IASS International Symposium*, Vol.2, Italy, pp.1085-1092, 1995.

[6] Qiao, F., Hagiwara, N. and Matsui, T., On the Relation between Absorbed Energy and Dynamic Collapse of a Single-Layer Shallow Latticed Domes, *Journal of Structural and Construction Engineering (Transactions of AIJ)*, No.531, pp.117-124, 2000.

[7] SPACE; SPace frame Analysis package for Civil Engineers, researchers and students, http://wwwra.meijo-u.ac.jp/labs/ra007/space/index.htm.

[8] Ogawa, K., Inoue, K. and Nakashima, M., A Study of Earthquake Input Energy Causing Damages in Structures, *Journal of Structural and Construction Engineering (Transactions of AIJ)*, No.530, pp.177-184, 2000.